JOURNAL OF AIRCRAFT
Vol. 44, No. 2, March–April 2007

Time-Area-Averaged Momentum Stream Tube Model for Flapping Flight

Tianshu Liu*
Western Michigan University, Kalamazoo, Michigan 49008

DOI: 10.2514/1.23660

This paper formulates a time-area-averaged momentum stream tube model to provide the useful functional relations for the cruise velocity, power, and propulsive efficiency in forward flapping flight. This model is a direct generalization of the classical actuator disk theory by taking into account the effects of the unsteadiness and spatial nonuniformity of velocity in a momentum stream tube. It is found that the functional relation for the time-area-averaged power required in flapping flight is almost the same as that given by the classical lifting-line theory for a fixed wing. The flapping span efficiency is introduced, and its physical meaning and significant role in the power relation are interpreted. The flapping propulsive efficiency is related to the flapping span efficiency, normalized total fluctuating kinetic energy, and wing aspect ratio. The use of this model to fit the collected data for birds allows estimating the flapping span efficiency, parasite, and induced drag coefficients and propulsive efficiency.

Nomenclature

A = effective area of actuator disk or cross-section area of momentum stream tube
A_b = circular area of a diameter of wingspan
AR = wing aspect ratio
b = wingspan
$C_{D_{\text{Para}}}$ = parasite drag coefficient
C_L = lift coefficient
C_P = power coefficient
C_T = thrust coefficient
C_W = weight coefficient
C_{XY} = correlation coefficient between X and Y
D_{Para} = parasite drag
e_{flap} = flapping span efficiency
k = parameter describing the combined effect of azimuthal velocity fluctuation, spatial nonuniformity of velocity and viscous shear stress
$\langle L \rangle_{\text{tA}}$ = time-area-averaged lift
$\langle P \rangle_{\text{tA}}$ = time-area-averaged power
p = local pressure
p_0 = freestream pressure
p_1' = pressure fluctuation at actuator disk
p_2' = pressure fluctuation far downstream
r = parameter describing the combined effect of azimuthal velocity fluctuation and viscous shear stress
s = arc length of streamline
$\boldsymbol{s}$ = unit vector along momentum stream tube
s_1 = location of the actuator disk
s_2 = location far downstream
$\langle T \rangle_{\text{tA}}$ = time-area-averaged thrust
V = freestream velocity
$\boldsymbol{V}$ = velocity vector
V_1 = magnitude of $\boldsymbol{V}_1$
$\boldsymbol{V}_1$ = velocity vector at actuator disk
V_2 = magnitude of $\boldsymbol{V}_2$
$\boldsymbol{V}_2$ = asymptotic velocity vector deflected far downstream
V_s = velocity along stream tube
$\boldsymbol{v}'$ = fluctuating velocity
v_s' = fluctuating velocity along stream tube
W = weight
$\langle w \rangle_{\text{tA}}$ = time-area-averaged downwash
w' = fluctuating downwash
Δp = pressure jump across actuator disk
ΔV_1 = time-averaged velocity increment at actuator disk
ΔV_2 = time-averaged velocity increment far downstream
ε_1 = normalized axial fluctuating kinetic energy at actuator disk
ε_2 = correlation coefficient between axial velocity fluctuations at disk and far downstream
ε_3 = normalized total fluctuating kinetic energy far downstream
η = propulsive efficiency
ρ = air density
$\boldsymbol{\tau}$ = shear stress tensor

Introduction

THE momentum stream tube (MST) model, originally proposed by Rankine for propellers [1,2], has been used to estimate some important quantities such as power and characteristic velocities in helicopter aerodynamics [3,4] and flows in gas turbines [5]. Recently, after revisiting the MST model, Spalart [6] recovered the classical results on the induced power based on the momentum balance in a large domain with a far-field behavior known to a high order, without using either the quasi-one-dimensional argument or the assumption that the induced velocity is uniform at an actuator disk is required. Application of the MST model to hovering insect flight was explored by Ellington [7] and extended to forward flapping flight of birds and insects [8–10]. In particular, Ellington [7] improved the classical Rankine–Froude theory by introducing corrections for nonuniformity and periodic fluctuation of pressure based on a simple vortex model. Ellington's work focused on insect hovering flight in which the wake can be reasonably represented by an axial chain of circular vortex rings. For forward flight where the wake topology is complicated, however, existing MST models do not explicitly consider the effects of unsteadiness and spatial nonuniformity of velocity produced by the trailing vortex system. Therefore, a recurring question is whether or not steady or quasisteady MST models could be applied to a highly unsteady force generator like a flapping wing in forward flight. Clearly, a more general approach is desirable to incorporate the unsteadiness and spatial nonuniformity of velocity into a MST model. Furthermore, although the classical power-velocity relation for fixed-wing flight has been commonly adopted in the studies of bird flight [9,11,12], the

Received 5 March 2006; accepted for publication 3 October 2006.

*Associate Professor, Department of Mechanical and Aeronautical Engineering, College of Engineering and Applied Sciences, G-220, Parkview Campus; tianshu.liu@wmich.edu. Member AIAA.

legitimacy of direct application of this relation to an unsteady force generator (e.g., a flapping wing) is not quantitatively justified yet. To answer to these questions, the time-area-averaged MST model is formulated for a flapping wing by incorporating the effects of the unsteadiness and spatial nonuniformity of velocity. The time-area-averaged thrust, lift, power, and propulsive efficiency for flapping flight are calculated. The proposed time-area-averaging approach for forward flight can be similarly applied to hovering flight. Note that Ellington [7] used area average for nonuniformity and time average for unsteadiness separately, and then added the two corrections linearly. In this work, the time-area-averaging approach deals with the spatial nonuniformity and temporal unsteadiness altogether.

A physical scenario is that a flapping wing in level flight induces a sequence of impulse momentum fluxes associated with a trailing vortex system (a pair of undulated vortices for fast flight or a series of vortex rings for slow flight), which are deflected downward in a time-average sense. In the MST model, this scenario is approximated as a momentum stream tube driven by an actuator disk and at the same time deflected downward by the induction of a trailing vortex system. As shown in Fig. 1, in a time-average sense, the actuator disk produces the thrust by increasing the axial momentum across the disk, whereas the lift is generated as a result of deflecting the momentum stream tube by the downwash induced by the trailing vortex system [8]. The downwash has a side effect on flapping flight; it decreases the angle of attack of the incoming flow producing the induced drag. In this sense, the lift and induced drag are related by the common source: the downwash induced by a trailing vortex system. For the development of this work, the time-area-averaged Bernoulli's equation along a streamline tube is given, and then a time-area-averaged actuator disk model is built. Deflection of the momentum stream tube by the trailing vortex system is studied and the time-area-averaged thrust, lift, power, and propulsive efficiency are calculated. The significance of the time-area-averaged MST model is that it provides the useful functional relations for the time-area-averaged cruise velocity, power, and propulsive efficiency.

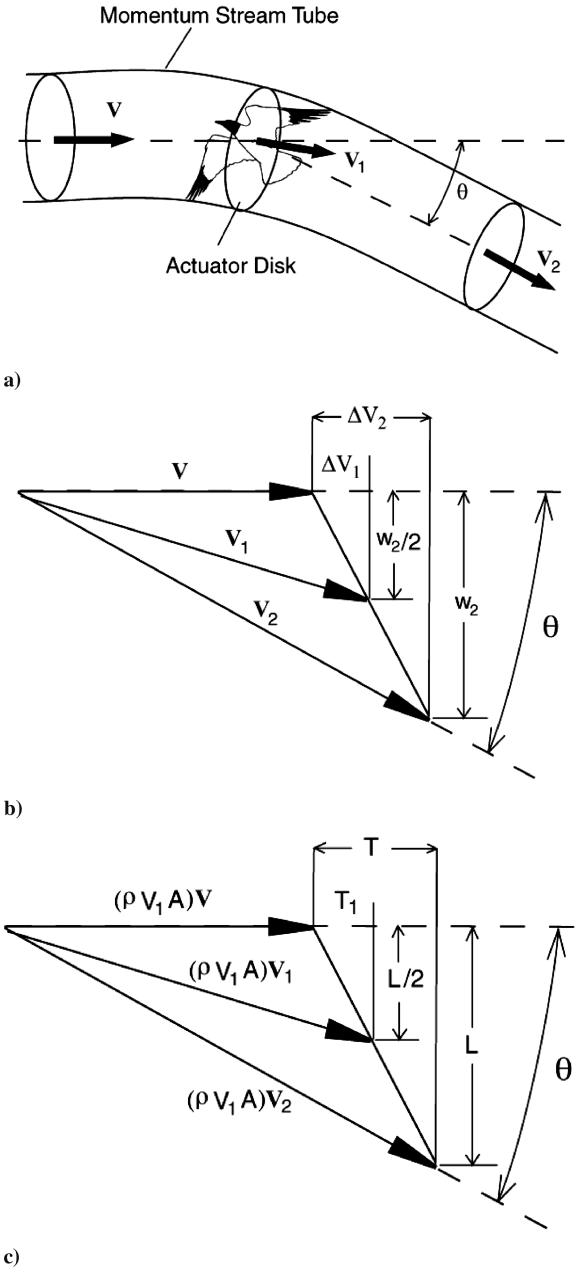

Fig. 1 a) Momentum stream tube; b) velocity vectors; c) momentum vectors (adapted from Templin [8]).

The time-area-averaged MST model is a simple lumped aerodynamic model for complicated flapping flight, in which the effects of the wing geometry and kinematics and velocity unsteadiness of the wake are collectively represented by some empirical parameters such as the flapping span efficiency and total fluctuating kinetic energy. This model cannot give the instantaneous lift, thrust, and power, and evaluate the effects of the reduced frequency and flapping amplitude. Hence, this approach gives limited but useful results complementary to more elaborated models such as quasisteady and unsteady lifting-line theories [13–17] and models based on prescribed trailing vortex structures [18–20].

Time-Area-Averaged Bernoulli's Equation

Consider the Navier–Stokes equations and the continuity equation for an incompressible flow

$$\rho\frac{\partial \boldsymbol{V}}{\partial t}+\frac{\rho}{2}\nabla(\boldsymbol{V}\cdot\boldsymbol{V})-\boldsymbol{V}\times(\nabla\times\boldsymbol{V})=-\nabla p+\nabla\cdot\boldsymbol{\tau} \tag{1}$$

$$\nabla\cdot\boldsymbol{V}=0 \tag{2}$$

Projection of Eq. (1) onto a streamline is

$$\rho\frac{\partial V_s}{\partial t}+\frac{\rho}{2}\nabla_s(\boldsymbol{V}\cdot\boldsymbol{V})=-\nabla_s p+\nabla\cdot\boldsymbol{\tau}_s-\kappa(\nabla s)\cdot\boldsymbol{\tau}_n \tag{3}$$

where $V_s=\boldsymbol{s}\cdot\boldsymbol{V}$ is the velocity along the tangential direction $\boldsymbol{s}$ of the streamline, $\nabla_s=\boldsymbol{s}\cdot\nabla$ is the gradient along the streamline, κ is the curvature of the streamline, and the vectors $\boldsymbol{\tau}_s=\tau_{ij}s_i$ and $\boldsymbol{\tau}_n=\tau_{ij}n_i$ are the projections of the viscous shear stress tensor onto the tangential and normal directions of the streamline, respectively. To obtain Eq. (3), the Frenet–Serret formulas $\partial s_j/\partial x_i=\kappa n_j\partial s/\partial x_i$ and vector relation $\boldsymbol{s}\cdot[\boldsymbol{V}\times(\nabla\times\boldsymbol{V})]=0$ along the streamline are used. The term $\kappa(\nabla s)\cdot\boldsymbol{\tau}_n$ is a product of a change of the normal shear stress along the streamline and the streamline curvature. For fast level flight, the instantaneous streamline curvature is generally small and the normal shear stress along the streamline does not drastically change. In this case, the term $\kappa(\nabla s)\cdot\boldsymbol{\tau}_n$ can be neglected.

Applying the long-term time average $\langle\cdot\rangle_t=\lim_{T\to\infty}T^{-1}\int_0^T\cdot\mathrm{d}t$ to Eq. (3), when the integration of V_s along the streamline is finite, we have

$$\frac{\partial}{\partial s}\left(\frac{\rho}{2}\langle\boldsymbol{V}\cdot\boldsymbol{V}\rangle_t+\langle p\rangle_t\right)=\nabla\cdot\langle\boldsymbol{\tau}_s\rangle_t \tag{4}$$

Further, the area average $\langle\cdot\rangle_A=A^{-1}\int_A\cdot\mathrm{d}A$ is introduced. Equation (4) is integrated over an elemental volume of the tube $A\partial s$ and it is assumed that $\partial A/\partial s$ is sufficiently small such that all terms related to $\partial A/\partial s$ can be neglected. Using the Gauss's theorem and imposing the zero-flux condition for $\boldsymbol{\tau}_s$ in the normal direction of the peripheral surface of the tube, we obtain

$$\frac{\rho}{2}\langle\boldsymbol{V}\cdot\boldsymbol{V}\rangle_{\mathrm{tA}}+\langle p\rangle_{\mathrm{tA}}-\langle|\boldsymbol{\tau}_s|\rangle_{\mathrm{tA}}=\text{const} \tag{5}$$

where the operator $\langle\cdot\rangle_{tA} = \langle\langle\cdot\rangle_t\rangle_A$ is the time-area average. Clearly, Eq. (5) is a time-area-averaged Bernoulli's equation along a streamline tube. Furthermore, when $\boldsymbol{V}$ is decomposed into a time-averaged component along a streamline tube and fluctuating velocity with zero mean, that is $\boldsymbol{V} = \langle V_s\rangle_t + \boldsymbol{v}'$, Eq. (5) becomes

$$\frac{\rho}{2}C_{V_sV_s}(s)\langle V_s\rangle_{tA}^2 + \frac{\rho}{2}\langle|\boldsymbol{v}'|^2\rangle_{tA} + \langle p\rangle_{tA} - \langle|\boldsymbol{\tau}_s|\rangle_{tA} = \text{const} \tag{6}$$

where $C_{V_sV_s}(s) = \langle\langle V_s\rangle_t^2\rangle_A/\langle V_s\rangle_{tA}^2$ is an autocorrelation coefficient depending on the velocity profile across the stream tube. Here, $\boldsymbol{v}'$, which is not particularly prescribed, should have a zero long-term time mean. In addition, $\boldsymbol{v}'$ cannot be large relative to the flight velocity to satisfy the condition of small streamline curvature. Similarly, integration of the continuity equation (2) over an elemental volume of the tube $A\partial s$ yields $A\langle V_s\rangle_{tA} = 0$.

Time-Area-Averaged Actuator Disk

Typically, a stream tube is divided into two parts by an actuator disk simulating the action of an unsteady force generator. The normal of the actuator disk is parallel to the freestream velocity $V\boldsymbol{s}$, generating an increase of the momentum and kinetic energy along $\boldsymbol{s}$ of the stream tube. On approaching the disk, the axial velocity along the stream tube rises to $(V + \Delta V_1)\boldsymbol{s} + \boldsymbol{v}'(s_1, t)$ and the static pressure falls from the undisturbed p_0 to p, where $\boldsymbol{v}'(s_1, t)$ is the fluctuating velocity at the disk. The axial velocity remains $(V + \Delta V_1)\boldsymbol{s} + \boldsymbol{v}'(s_1, t)$ across the disk, but approaches to $(V + \Delta V_2)\boldsymbol{s} + \boldsymbol{v}'(s_2, t)$ far downstream. In contrast to the continuity of velocity, the pressure jumps from p to $p + \Delta p + p_1'(t)$ across the disk, and then reduces to $p_0 + p_2'(t)$ far downstream.

According to the time-area-averaged Bernoulli's equation Eq. (6), we have the total pressure head upstream of the actuator disk

$$H_0 = p_0 + \frac{\rho}{2}V^2 = \langle p\rangle_{tA}(s_1) + \frac{\rho}{2}C_{V_sV_s}(s_1)\langle V + \Delta V_1\rangle_{tA}^2 + \frac{\rho}{2}\langle|\boldsymbol{v}'|^2\rangle_{tA}(s_1) - \langle|\boldsymbol{\tau}_s|\rangle_{tA}(s_1) \tag{7}$$

and the total pressure head immediately behind the actuator disk

$$H_1 = p_0 + \frac{\rho}{2}C_{V_sV_s}(s_2)\langle V + \Delta V_2\rangle_{tA}^2 + \frac{\rho}{2}\langle|\boldsymbol{v}'|^2\rangle_{tA}(s_2) - \langle|\boldsymbol{\tau}_s|\rangle_{tA}(s_2) = \langle p\rangle_{tA}(s_1) + \langle\Delta p\rangle_{tA}(s_1) + \frac{\rho}{2}C_{V_sV_s}(s_1)\langle V + \Delta V_1\rangle_{tA}^2 + \frac{\rho}{2}\langle|\boldsymbol{v}'|^2\rangle_{tA}(s_1) - \langle|\boldsymbol{\tau}_s|\rangle_{tA}(s_1) \tag{8}$$

The difference $H_1 - H_0$ leads to the time-area-averaged pressure jump across the disk

$$\langle\Delta p\rangle_{tA}(s_1) = \frac{\rho}{2}[C_{V_sV_s}(s_2) - 1]V^2 + \frac{\rho}{2}C_{V_sV_s}(s_2)(2V + \langle\Delta V_2\rangle_{tA})\langle\Delta V_2\rangle_{tA} + \frac{\rho}{2}\langle|\boldsymbol{v}'|^2\rangle_{tA}(s_2) - \langle|\boldsymbol{\tau}_s|\rangle_{tA}(s_2) \tag{9}$$

From Eq. (9), the time-area-averaged thrust is $\langle T\rangle_{tA} = A\langle\Delta p\rangle_{tA}(s_1)$, where A is the effective area of the actuator disk. On the other hand, based on the rate of increase of the axial momentum, the time-area-averaged thrust is given by

$$\langle T\rangle_{tA} = A\rho\left[V\langle\Delta V_2\rangle_{tA} + C_{\Delta V_1\Delta V_2}\langle\Delta V_1\rangle_{tA}\langle\Delta V_2\rangle_{tA} + \left\langle v_s'^2\right\rangle_{tA}(s_2)\right] \tag{10}$$

where $v_s' = \boldsymbol{s}\cdot\boldsymbol{v}'(s_2, t)$ is the projection of the fluctuating velocity along the stream tube and the correlation coefficient is defined as $C_{\Delta V_1\Delta V_2} = \langle\Delta V_1\Delta V_2\rangle_{tA}/\langle\Delta V_1\rangle_{tA}\langle\Delta V_2\rangle_{tA}$. A direct comparison of Eq. (9) with Eq. (10) leads to the following relation:

$$C_{\Delta V_1\Delta V_2}\langle\Delta V_1\rangle_{tA} = 0.5C_{V_sV_s}(s_2)\langle\Delta V_2\rangle_{tA} + 0.5[C_{V_sV_s}(s_2) - 1]V^2\langle\Delta V_2\rangle_{tA}^{-1} + [C_{V_sV_s}(s_2) - 1]V + r\langle\Delta V_2\rangle_{tA} \tag{11}$$

where the nondimensional parameter r is defined as

$$r = \langle\Delta V_2\rangle_{tA}^{-2}\left\{0.5[\langle|\boldsymbol{v}'|^2\rangle_{tA}(s_2) - 2\left\langle v_s'^2\right\rangle_{tA}(s_2)\right] - \rho^{-1}\langle|\boldsymbol{\tau}_s|\rangle_{tA}(s_2)\right\} \tag{12}$$

The term $\langle|\boldsymbol{v}'|^2\rangle_{tA}(s_2) - 2\langle v_s'^2\rangle_{tA}(s_2)$ in Eq. (12) is the azimuthal kinetic fluctuating energy plus a difference between the fluctuating kinetic energies along the radial and axial directions in the stream tube. If the fluctuating kinetic energies along the radial and axial directions are approximately equal, it mainly describes the azimuthal velocity fluctuation far downstream. Thus, r collectively describes the effects of the azimuthal velocity fluctuation and viscous shear stress.

For $\langle\Delta V_2\rangle_{tA}/V \ll 1$ in fast forward flight, the correlation coefficient $C_{V_sV_s}(s_2)$ is approximated by $C_{V_sV_s}(s_2) \approx 1 + (C_{\Delta V_2\Delta V_2} - 1)\langle\Delta V_2\rangle_{tA}^2/V^2$, where the autocorrelation coefficient related to the velocity change is introduced. Note that the approximation $\langle\Delta V_2\rangle_{tA}/V \ll 1$ is not good for slow flight and hovering flight. Hence, for fast flight, a relation between the time-area-averaged velocity increments $\langle\Delta V_1\rangle_{tA}$ at the actuator disk and $\langle\Delta V_2\rangle_{tA}$ far downstream is

$$\langle\Delta V_1\rangle_{tA} = 0.5k\langle\Delta V_2\rangle_{tA} \tag{13}$$

where $k = (C_{\Delta V_2\Delta V_2} + 2r)/C_{\Delta V_1\Delta V_2}$ is a nondimensional parameter. Equation (13) is a fundamental relation in the time-area-averaged MST model. The classical result $\Delta V_1 = 0.5\Delta V_2$ in previous publications [2,3,8] is the special form of Eq. (13) for $C_{\Delta V_2\Delta V_2} = 1$, $C_{\Delta V_1\Delta V_2} = 1$ and $r = 0$ in a steady and uniform momentum stream tube. The correlation coefficients $C_{\Delta V_2\Delta V_2}$ and $C_{\Delta V_1\Delta V_2}$ describe the effects of the nonuniformity of velocity in the stream tube. For a uniform momentum stream tube, these correlation coefficients are $C_{\Delta V_2\Delta V_2} = 1$ and $C_{\Delta V_1\Delta V_2} = 1$. The physical meaning of the parameter k is clear, which describes the combined effect of the azimuthal velocity fluctuation, spatial nonuniformity of velocity and viscous shear stress. In certain sense, the role of the viscous shear stress can be interpreted as an effect of the nonuniformity of velocity associated with viscosity.

Deflection of Momentum Stream Tube by Trailing Vortex System

A momentum stream tube driven by an actuator disk is deflected by the induction of a trailing vortex system. The trailing vortex system induces $\langle w\rangle_{tA}$ as well as w'. The downwash produces the deflection of the momentum stream tube, which generates the lift. The time-area-averaged downwash velocity at the actuator disk induced by the semi-infinite vortex system is just half of that far downstream induced by the infinite vortex system. This is another important relation serving as the foundation of the MST model along with Eq. (13). As pointed out before, Eq. (13) gives the relation between the longitudinal component $\langle\Delta V_1\rangle_{tA}$ of a change in velocity across the disk and the longitudinal velocity change $\langle\Delta V_2\rangle_{tA}$ far downstream. The relationship between the instantaneous velocity and momentum vectors in the stream tube is illustrated in Fig. 1.

The time-area-averaged thrust is given by the change of the momentum flux far downstream, that is,

$$\langle T\rangle_{tA} = \rho A\langle V_1(V_2\cos\theta - V)\rangle_{tA} = \rho A[C_{V_1\Delta V_2}\langle V_1\rangle_{tA}\langle\Delta V_2\rangle_{tA} + \langle v_s'(s_1)v_s'(s_2)\rangle_{tA}] \tag{14}$$

where the correlation coefficient $C_{V_1\Delta V_2}$ is defined as $C_{V_1\Delta V_2} = \langle\langle V_1\rangle_t\langle\Delta V_2\rangle_t\rangle_A/\langle V_1\rangle_{tA}\langle\Delta V_2\rangle_{tA}$. The change of the momentum flux immediately behind the actuator disk is

$$\langle T_1\rangle_{tA} = \rho A\left[C_{V_1\Delta V_1}\langle V_1\rangle_{tA}\langle\Delta V_1\rangle_{tA} + \left\langle v_s'^2\right\rangle_{tA}(s_1)\right] \tag{15}$$

where the correlation coefficient $C_{V_1\Delta V_1}$ is defined as $C_{V_1\Delta V_1} = \langle\langle V_1\rangle_t\langle\Delta V_1\rangle_t\rangle_A/\langle V_1\rangle_{tA}\langle\Delta V_1\rangle_{tA}$. Substitution of Eqs. (13) and (14) into Eq. (15) yields a relation

$$\langle T_1\rangle_{tA} = 0.5\alpha_1\langle T\rangle_{tA} + \rho A\left[\left\langle v_s'^2\right\rangle_{tA}(s_1) - 0.5\alpha_1\langle v_s'(s_1)v_s'(s_2)\right\rangle_{tA}\right] \tag{16}$$

where the parameter α_1 is defined as $\alpha_1 = kC_{V_1\Delta V_1}/C_{V_1\Delta V_2}$ and its physical meaning is the same as the parameter k. Further, introducing the nondimensional parameters $\varepsilon_1 = \langle\Delta V_2\rangle_{tA}^{-2}\langle v_s'^2\rangle_{tA}(s_1)$ and $\varepsilon_2 = \langle\Delta V_2\rangle_{tA}^{-2}\langle v_s'(s_1)v_s'(s_2)\rangle_{tA}$ and using the first-order approximation $\langle\Delta V_2\rangle_{tA} \approx \langle T\rangle_{tA}/\rho AC_{V_1\Delta V_2}\langle V_1\rangle_{tA}$, we obtain a relation between the changes of the momentum fluxes $\langle T_1\rangle_{tA}$ at the actuator disk and $\langle T\rangle_{tA}$ far downstream

$$\langle T_1\rangle_{tA} = 0.5\alpha_1\langle T\rangle_{tA} + \alpha_2\langle T\rangle_{tA}^2/(\rho A)^2\langle V_1\rangle_{tA}^2 \tag{17}$$

where the parameter α_2 is defined as $\alpha_2 = (\varepsilon_1 - 0.5\alpha_1\varepsilon_2)/C_{V_1\Delta V_2}^2$. As shown below, Eq. (17) is a useful intermediate relation to calculate the relative velocities at the actuator and far downstream along the stream tube. According to their definitions, the parameter ε_1 is the normalized axial fluctuating kinetic energy along the stream tube, whereas ε_2 is the correlation coefficient between the axial velocity fluctuations at the actuator disk and far downstream. Because the parameter α_2 is a combination of ε_1, ε_2 and α_1, it represents the combined effect of the velocity fluctuations, spatial nonuniformity of velocity and viscous shear stress.

As illustrated in Fig. 1, the time-area-averaged momentum fluxes along the stream tube at three locations (upstream, actuator disk, and far downstream) are, respectively,

$$\langle\rho AV_1V\rangle_{tA} = \rho AV\langle V_1\rangle_{tA} \tag{18}$$

$$\langle\rho AV_1V_1\rangle_{tA} = \rho A\left[C_{V_1V_1}\langle V_1\rangle_{tA}^2 + \left\langle v_s'^2\right\rangle_{tA}(s_1)\right] \approx \rho A[C_{V_1V_1}\langle V_1\rangle_{tA}^2 + \left(\varepsilon_1/C_{V_1\Delta V_2}^2\right)\langle T\rangle_{tA}^2/(\rho A)^2\langle V_1\rangle_{tA}^2\Big] \tag{19}$$

$$\langle\rho AV_1V_2\rangle_{tA} = \rho A[C_{V_1V_2}\langle V_1\rangle_{tA}\langle V_2\rangle_{tA} + \langle v_s'(s_1)v_s'(s_2)\rangle_{tA}] \approx \rho A\left[C_{V_1V_2}\langle V_1\rangle_{tA}\langle V_2\rangle_{tA} + \left(\varepsilon_2/C_{V_1\Delta V_2}^2\right)\langle T\rangle_{tA}^2/(\rho A)^2\langle V_1\rangle_{tA}^2\right] \tag{20}$$

where $C_{V_1V_1} = \langle\langle V_1\rangle_t^2\rangle_A/\langle V_1\rangle_{tA}^2$ and $C_{V_1V_2} = \langle\langle V_1\rangle_t\langle V_2\rangle_t\rangle_A/\langle V_1\rangle_{tA}\langle V_2\rangle_{tA}$ are the correlation coefficients. The time-area-averaged lift is equal to the change of the normal momentum flux induced by the downwash w far downstream, that is,

$$\langle L\rangle_{tA} = \langle\rho AV_1w(s_2)\rangle_{tA} = \rho A(\langle\langle V_1\rangle_t\langle w\rangle_t(s_2)\rangle_A + \langle v_s'(s_1)w'(s_2)\rangle_{tA}) \tag{21}$$

Also, as indicated in Fig. 1, there is a geometrical relation between the momentum vectors

$$\langle\rho AV_1V_1\rangle_{tA}^2 = (\langle\rho AV_1V\rangle_{tA} + \langle T_1\rangle_{tA})^2 + (\langle L\rangle_{tA}/2)^2 \tag{22}$$

The effective area of an actuator disk is not clearly defined for a flapping wing unlike for a propeller, and the shape of an actuator disk is unknown. The effective actuator disk area is modeled by $A = e_{flap}\pi b^2/4$. The nominal definition of e_{flap} is a ratio between the effective actuator disk area and full circular area of a diameter of the wingspan. Physically speaking, the flapping span efficiency depends on not only the wing geometry, but also flapping kinematics. Here, the term "span efficiency" is adopted for e_{flap} because it plays the same role as the Oswald efficiency for fixed-wing aircraft in the power relation for level flight (this will be discussed later). In the MST model, the nondimensional coefficients for the thrust and lift, $C_T = \langle T\rangle_{tA}/(\rho V^2A_b/2)$ and $C_L = \langle L\rangle_{tA}/(\rho V^2A_b/2)$, are usually defined based on $A_b = \pi b^2/4 = A/e_{flap}$, the area of a circular disk of a diameter b rather than the wing area. Therefore, the thrust and lift coefficients depend on the flapping span efficiency.

Substitution of Eqs. (17–21) into Eq. (22) leads to a nonlinear algebraic equation for the time-area-averaged velocity at the actuator disk along the stream tube

$$\left(\frac{\langle V_1\rangle_{tA}}{V}\right)^4 - D_2\left(\frac{\langle V_1\rangle_{tA}}{V}\right)^2 - D_1\left(\frac{\langle V_1\rangle_{tA}}{V}\right) - D_0 = 0 \tag{23}$$

where the coefficients are defined as

$$D_0 = \frac{1}{4C_{V_1V_1}^2}\left[\left(\frac{C_L}{2e_{flap}}\right)^2 + \left(\frac{\alpha_1C_T}{2e_{flap}} + 2\alpha_2q\right)^2 - \left(\frac{2\varepsilon_1q}{C_{V_1\Delta V_1}^2}\right)^2\right]$$

$$D_1 = \frac{2}{C_{V_1V_1}^2}\left(\frac{\alpha_1C_T}{4e_{flap}} + \alpha_2q\right)$$

$$D_2 = \frac{1}{C_{V_1V_1}^2} - \frac{2\varepsilon_1q}{C_{V_1V_1}C_{V_1\Delta V_1}^2}$$

$$q = \left(\frac{C_T}{2e_{flap}\langle V_1\rangle_{tA}V^{-1}}\right)^2$$

In fact, because the above coefficients depend on C_T and C_L that are related to the unknown $\langle V_1\rangle_{tA}/V$, Eq. (23) is a more complicated equation even though it is formally written as a fourth-order algebraic equation. In general, Eq. (23) should be solved iteratively with Eqs. (25–27) for $\langle V_2\rangle_{tA}/V$, C_T, and C_L altogether. Note that Eq. (23) is a generalization of that given by Templin [8] in his steady and uniform MST model.

Another geometrical relation between the momentum vectors is

$$\langle\rho AV_1V_2\rangle_{tA}^2 = (\langle\rho AV_1V\rangle_{tA} + \langle T\rangle_{tA})^2 + \langle L\rangle_{tA}^2 \tag{24}$$

and the corresponding nondimensional form is

$$4e_{flap}^2\left(C_{V_1V_2}\frac{\langle V_1\rangle_{tA}}{V}\frac{\langle V_2\rangle_{tA}}{V} + \frac{\varepsilon_2q}{C_{V_1\Delta V_1}^2}\right)^2 = \left(2e_{flap}\frac{\langle V_1\rangle_{tA}}{V} + C_T\right)^2 + C_L^2 \tag{25}$$

Once the relative velocity $\langle V_1\rangle_{tA}/V$ at the actuator disk is obtained by solving Eq. (23), the asymptotic velocity $\langle V_2\rangle_{tA}/V$ far downstream is readily given by Eq. (25). Then, these relative velocities are used to calculate the power and thrust coefficients.

Time-Area-Averaged Thrust and Lift

From Eq. (15), we know the thrust coefficient

$$C_T = \frac{\langle T\rangle_{tA}}{\rho A_bV^2/2} = 2e_{flap}\left(C_{V_1\Delta V_2}\frac{\langle V_1\rangle_{tA}\langle\Delta V_2\rangle_{tA}}{V^2} + \frac{\langle v_s'(s_1)v_s'(s_2)\rangle_{tA}}{V^2}\right) \tag{26}$$

where the first term is the quasisteady thrust and the second term is a two-point correlation of the velocity fluctuation along the stream tube. Similarly, from Eq. (21), the lift coefficient is

$$C_L = \frac{\langle L\rangle_{tA}}{\rho V^2A_b/2} = 2e_{flap}\left(\frac{\langle\langle V_1\rangle_t\langle w\rangle_t(s_2)\rangle_A}{V^2} + \frac{\langle v_s'(s_1)w'(s_2)\rangle_{tA}}{V^2}\right) \tag{27}$$

The two-point correlations $\langle v_s'(s_1)v_s'(s_2)\rangle_{tA}$ and $\langle v_s'(s_1)w'(s_2)\rangle_{tA}$ are related to the topology of the trailing vortex system. The organized topological structures of the bird's trailing vortex system, such as vortex rings and continuous constant-circulation vortices, have been proposed by Rayner [21,22] and Spedding et al. [23],

which could be useful for building vortex-dynamical models of flapping flight. The axial fluctuating velocity $v'_s(s_1)$ immediately behind the disk is periodic. For theoretical simplicity, the topological structure of the vortex system could be assumed to be spatially periodic and well organized, and therefore $v'_s(s_1)$ and $v'_s(s_2)$ or $w'(s_2)$ could be highly correlated. However, this scenario may not be realistic far downstream. In fact, due to the self-induction and mutual induction of the vortex structures, the highly undulated vortex system is unstable and becomes increasingly complicated in its topology far downstream. The induced velocity fluctuation $v'_s(s_2)$ or $w'(s_2)$ at a fixed location far downstream, in addition to the velocity fluctuation of small-scale turbulence, increasingly appears nonperiodic and chaotic. As a result, the two-point correlations $\langle v'_s(s_1)v'_s(s_2)\rangle_{\text{tA}}$ and $\langle v'_s(s_1)w'(s_2)\rangle_{\text{tA}}$ should decrease to zero far downstream, and the effects of the velocity fluctuations on the time-area-averaged lift and thrust are negligible.

Time-Area-Averaged Power

The time-area-averaged power required for flapping flight is given by

$$\langle P\rangle_{\text{tA}} = 0.5\rho A\left(\left\langle\langle V_1\rangle_t\langle V_2\rangle_t^2\right\rangle_A + \langle\langle V_1\rangle_t\langle|\boldsymbol{v}'|^2\rangle_t(s_2)\rangle_A - V^2\langle V_1\rangle_{\text{tA}}\right) \tag{28}$$

As an approximation, when $\langle V_1\rangle_t$ is assumed to be a top-hat function across the actuator disk immediately behind the disk, it can be decorrelated in the correlation terms in Eq. (28). Introducing the correlation coefficient $C_{V_2V_2} = \langle\langle V_2\rangle_t^2\rangle_A/\langle V_2\rangle_{\text{tA}}^2$, we have the power coefficient

$$C_P = \frac{\langle P\rangle_{\text{tA}}}{\rho A_b V^3/2} = e_{\text{flap}}\left(\frac{\langle V_1\rangle_{\text{tA}}}{V}\right)\left(C_{V_2V_2}\left(\frac{\langle V_2\rangle_{\text{tA}}}{V}\right)^2 + \frac{\langle|\boldsymbol{v}'|^2\rangle_{\text{tA}}(s_2)}{V^2} - 1\right) \tag{29}$$

The term $\langle|\boldsymbol{v}'|^2\rangle_{\text{tA}}(s_2)/V^2$ in Eq. (29) can be further written as $\varepsilon_3\langle\Delta V_2\rangle_{\text{tA}}^2/V^2$, where the parameter $\varepsilon_3 = \langle|\boldsymbol{v}'|^2\rangle_{\text{tA}}(s_2)/\langle\Delta V_2\rangle_{\text{tA}}^2$ is the normalized total fluctuating kinetic energy far downstream and $\langle\Delta V_2\rangle_{\text{tA}}/V$ is related to the thrust coefficient [see Eq. (32)].

Because a number of the correlation coefficients and parameters have been introduced in the above analysis, it is necessary to estimate them in fast flight. For $\langle\Delta V_2\rangle_{\text{tA}}/V \ll 1$ in fast flight, the estimates for the correlation coefficients and other relevant parameters are $C_{V_1V_1} = 1 + O(C_T^2)$, $C_{V_1V_2} = 1 + O(C_T^2)$, $C_{V_2V_2} = 1 + O(C_T^2)$, $C_{V_1\Delta V_1} = 1 + O(C_T)$, $C_{V_1\Delta V_2} = 1 + O(C_T)$, $\alpha_1 = k + O(C_T)$, and $\alpha_2 = \varepsilon_1 - k\varepsilon_2/2 + O(C_T)$. Accordingly, the estimates for the coefficients in the algebraic equation (23) are $D_0 = [C_L^2 + (kC_T)^2]/16e_{\text{flap}}^2 + O(C_T^3)$, $D_1 = kC_T/2e_{\text{flap}} + O(C_T^2)$, and $D_2 = 1 + O(C_T^2)$. We take a close look at the correlation coefficients $C_{\Delta V_2\Delta V_2}$ and $C_{\Delta V_1\Delta V_2}$ that depend on the velocity profiles across the momentum stream tube. When the time-averaged velocity at the disk $\langle V_1\rangle_t$ is assumed to be a top-hat function, we know $C_{\Delta V_1\Delta V_2} = 1$. The coefficient $C_{\Delta V_2\Delta V_2} = \langle(\Delta V_2)^2\rangle_{\text{tA}}/\langle\Delta V_2\rangle_{\text{tA}}^2$ is interesting because it is related to the jetlike flow far downstream of the momentum stream tube. In a sense of the long-term time average, the Reynolds stress can be introduced to estimate the effect of the velocity fluctuation generated by a flapping wing on the time-averaged velocity profile. The flow far downstream may asymptotically approach a self-preserving state. Furthermore, the eddy viscosity is assumed to be constant across the momentum stream tube, and thus the motion equations are mathematically analogous to those for laminar flow. Hence, for $\langle\Delta V_2\rangle_{\text{tA}}/V \ll 1$, we adopt the self-similar solution for the laminar axisymmetric jetlike flow $\langle\Delta V_2\rangle_t = U_r\exp[-(y/l_r)^2]$ to describe the time-averaged velocity profile [24], where y is the radial coordinate, and U_r and l_r are the appropriate velocity and length scales of the jet. Using this similar velocity profile, we give an estimate $C_{\Delta V_2\Delta V_2} = e_{\text{flap}}b^2/8l_r^2$, representing a ratio between the effective area of an actuator disk and the characteristic area of the jet far downstream.

For level cruising flight where $C_L = C_W$, those correlation coefficients related to V_1 and V_2 are approximately one. The solutions to Eqs. (23) and (25) for $\langle V_1\rangle_{\text{tA}}/V$ and $\langle V_2\rangle_{\text{tA}}/V$ mainly depend on the flapping span efficiency e_{flap}, the parameter $k = (C_{\Delta V_2\Delta V_2} + 2r)/C_{\Delta V_1\Delta V_2}$, and the parameters ε_1 and ε_2 representing the fluctuating kinetic energy. Thus, a functional relation is $\langle P\rangle_{\text{tA}} = f(V, W, \rho, A_b, C_T, e_{\text{flap}}, k, \varepsilon_1, \varepsilon_2, \varepsilon_3)$ for the time-area-averaged power required for flapping flight.

To examine the effects of these parameters to the power relation, the time-area-averaged power has been computed by solving Eqs. (23), (25–27), and (29) altogether. It is indicated that the effects of the parameters k, ε_1, ε_2, and ε_3 on the time-area-averaged power are small. The relative error in calculations of the power coefficient C_P due to a change of $k = 1$–6 is less than 2% when the parameters ε_1, ε_2, and ε_3 are set at zero. The relative error in calculation of the power coefficient C_P due to the fluctuating velocities ($\varepsilon_1 = 0$–1, $\varepsilon_2 = 0$, and $\varepsilon_3 = 0$–6) is less than 0.1% for $k = 1$. These results indicate that the functional relationship for the time-area-averaged power coefficient is not sensitive to the parameters k, ε_1, ε_2, and ε_3. Hence, we assume that k is one and ε_1, ε_2, and ε_3 equal zero without a risk of producing a drastically different result. Therefore, a dimensional analysis gives a functional relation $C_P = f(C_W, C_T, e_{\text{flap}})$, where $C_P = \langle P\rangle_{\text{tA}}/(\rho A_b V^3/2)$, $C_T = \langle T\rangle_{\text{tA}}/(\rho V^2 A_b/2)$, and $C_W = W/(\rho V^2 A_b/2)$ are the coefficients for the power, thrust, and weight, respectively.

Because of the nonlinear nature of the algebraic equation Eq. (23), an analytical solution cannot be found for the power required for flapping flight. Instead, numerical computations were conducted to evaluate the power coefficient C_P in a parametric space $(C_W, C_T, e_{\text{flap}})$. Fitting the computational results, we reduce the following functional relation:

$$C_P = C_T + \frac{C_W^2}{4e_{\text{flap}}^{0.9}} = C_{D_{\text{Para}}} + \frac{C_W^2}{4e_{\text{flap}}^{0.9}} \tag{30}$$

The two terms on the right-hand side of Eq. (30) are the parasite (zero-lift) power and lift-induced power, respectively. Interestingly, the apparently different formulation of the time-area-averaged MST model for a flapping wing gives the almost same functional relation for the power as that given by the classical lifting-line theory for a fixed wing [25]. The difference is that the exponent of e_{flap} is 0.9 rather than one. This small deviation from the lifting-line theory can also be described by adding a correction term for the induced power [26]. Qualitatively, it is not unexpected that the power required is decomposed into the parasite and induced powers for both fixed-wing flight and flapping flight. Nevertheless, the flapping span efficiency e_{flap} in Eq. (30) is a more relevant parameter to flapping flight. Although the flapping span efficiency is analogous to the Oswald efficiency for fixed-wing flight, it has a different physical meaning, which is nominally defined as a ratio between the effective actuator disk area and full circular area and depends on the wing geometry and flapping kinematics. This is a subtle but important difference, and the true meaning of e_{flap} should be carefully stressed when data of flapping flight (bird flight) are interpreted for comparison with fixed-wing flight.

When the power-velocity relation for fixed-wing aircraft was initially used by researchers to estimate the parasite drag and Oswald efficiency by fitting measured data for birds, it was puzzling that the extracted span efficiency (0.2–0.7) for birds was not only divergent, but also generally lower than an assumed value (0.8–0.9) directly adopted from the aerodynamic theory of fixed-wing aircraft [12]. A lower span efficiency indicates a higher induced drag coefficient associated with bird flight. These "unexpected" results are hard to explain based on the original meaning of the Oswald efficiency that is the efficiency relative to the elliptical lift distribution. In fact, according to Eq. (30), e_{flap}, rather than the Oswald efficiency, should be used for a reasonable explanation. The flapping span efficiency, which is nominally defined as a ratio between the effective actuator disk area and the full circular area of a wingspan, depends on not only the wing geometry (morphology), but also the flapping kinematics.

In addition, the effective actuator disk area could be significantly smaller than the full circular area of a wingspan. Therefore, a value of the e_{flap} could be smaller, and it might considerably vary for different birds. Furthermore, due to wing morphing, e_{flap} may be velocity dependent in bird flight.

The typical power-velocity curve given by Eq. (30) is U shaped, and it has two characteristic velocities: the minimum power velocity V_{mp} and maximum range velocity V_{mr}. The maximum range velocity (the cruise velocity) V_{mr} corresponds to the tangential point of a line from the origin to the power curve, at which a migrating bird covers the longest distance for a given amount of energy. The corresponding powers at V_{mp} and V_{mr} are denoted by P_{mp} and P_{mr}, respectively. The general relations $V_{\text{mr}} = 1.35V_{\text{mp}}$ and $P_{\text{mr}} = 1.146P_{\text{mp}}$ can be reduced from Eq. (30). Consider a typical bird whose geometrical quantities obey the scaling laws $b = 0.506W^{1/3}$, $\bar{c} = 0.0646W^{1/3}$, $S_{\text{wing}} = 0.0327W^{2/3}$, and $AR = 7.83$ [26], where W is the bird weight. By adjusting the two free parameters $C_{D_{\text{Para}}}$ and e_{flap}, the maximum range power and velocity can be calculated as a function of W to fit simultaneously both the data collected by Greenewalt [12] for P_{mr} and data collected by Tennekes [27] for V_{mr}. Thus, based on the calculations, we obtain $e_{\text{flap}} = 0.463$ and $C_{D_{\text{Para}}} = 0.0055$ for birds and the corresponding correlations $P_{\text{mr}} = 0.9542W^{1.161}$ and $V_{\text{mr}} = 9.067W^{0.162}$. The flapping span efficiency $e_{\text{flap}} = 0.463$ is lower than the Oswald efficiency of a typical fixed-wing aircraft.

As shown in Fig. 2a, $P_{\text{mr}} = 0.9542W^{1.161}$ is compared well with Greenewalt's data for birds [12] and is close to Rayner's correlation

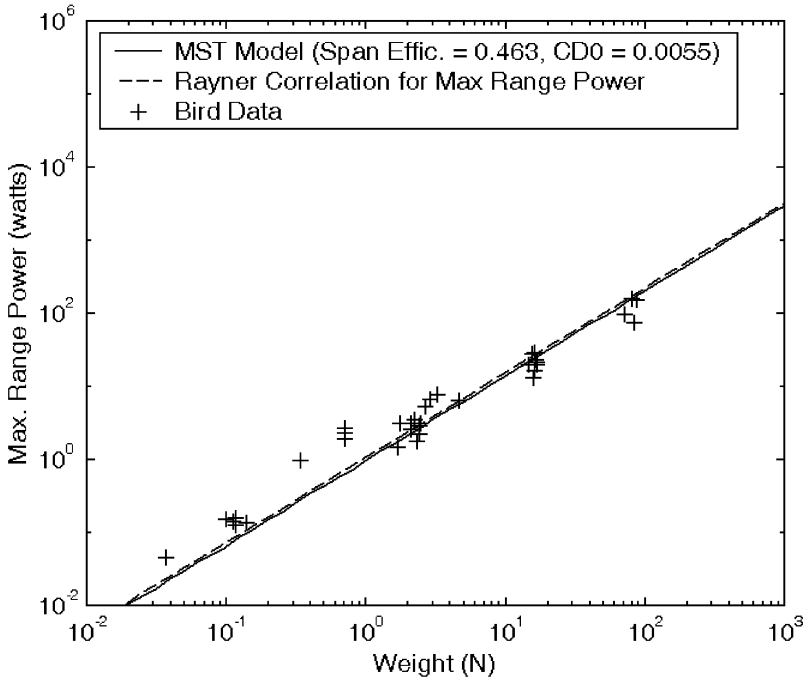

a)

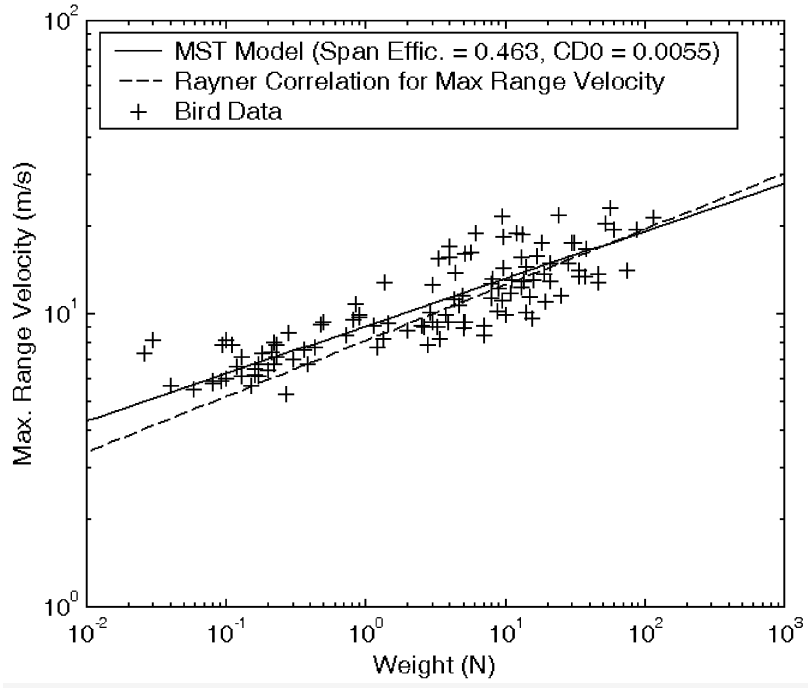

b)

Fig. 2 The maximum range power and velocity as a function of the bird weight.

$P_{\text{mr}} = 1.0564W^{1.161}$ given by the continuous vortex ring theory [28]. At the same time, as shown in Fig. 2b, the maximum range velocity $V_{\text{mr}} = 9.067W^{0.162}$ is basically consistent with Tennekes' [27] data and Rayner's [28] correlation $V_{\text{mr}} = 8.0952W^{0.19}$. Note that $C_{D_{\text{Para}}}$, which generally depends on Reynolds number, is treated as a constant parameter in the time-area-average sense over a range of Reynolds numbers for birds. Therefore, if Tennekes' data and Greenewalt's data represent a statistical ensemble of the data for a heterogeneous group of birds, $e_{\text{flap}} = 0.463$ and $C_{D_{\text{Para}}} = 0.0055$ can be considered as the ensemble average values for birds. Further, the parasite drag coefficient $C_{D_{\text{Para}}} = 0.0055$ for birds based on the disk area A_b is converted to the conventional drag coefficient $C_{D_{\text{Para}},S_{\text{wing}}}$ based on the wing area S_{wing} by multiplying a factor $\pi AR/4$. For a typical bird with $AR = 7.83$, we have $C_{D_{\text{Para}},S_{\text{wing}}} = 0.0344$. Direct measurement of the drag of a flying bird or flapping wing is difficult because the thrust and drag cannot be cleanly separated from the measured force in the freestream direction. Limited data for several gliding birds whose wings were fixed indicate $C_{D_{\text{Para}},S_{\text{wing}}} =$ 0.01–0.024 [12].

To estimate the induced drag coefficient of birds in cruise flight based on the wing area $C_{D_{\text{In}},S_{\text{wing}}} = C^2_{W,S_{\text{wing}}}/(\pi AR e_{\text{flap}})$, using the scaling laws $V_{\text{mr}} = 8.98W^{1/6}$, $S_{\text{wing}} = 0.0327W^{2/3}$, and $AR = 7.83$ [26], we have $C_{D_{\text{In}},S_{\text{wing}}} = 0.0193/e_{\text{flap}}$ for the air density of 1.21 kg/m^3. For $e_{\text{flap}} = 0.463$, the induced drag coefficient is $C_{D_{\text{In}},S_{\text{wing}}} = 0.0417$, which is comparable to the parasite drag coefficient of birds $C_{D_{\text{Para}},S_{\text{wing}}} = 0.0344$. Thus, in a statistical sense of scaling, the total drag coefficient for birds is $C_{D,S_{\text{wing}}} = C_{D_{\text{Para}},S_{\text{wing}}} + C_{D_{\text{In}},S_{\text{wing}}} = 0.076$. The induced drag and parasite drag roughly equally contribute the total drag of birds.

Time-Area-Averaged Propulsive Efficiency

To estimate the time-area-averaged propulsive efficiency $\eta = C_T/C_P$, some approximations are used in Eqs. (26) and (29) for fast flight, that is, $C_{V_2V_2} = 1 + O(C_T^2) \approx 1$, $C_{V_1\Delta V_2} = 1 + O(C_T) \approx 1$, $\langle V_2\rangle_{\text{tA}}/V \approx 1 + \langle \Delta V_2\rangle_{\text{tA}}/V$, and $\langle V_1\rangle_{\text{tA}}/V \approx 1 + \langle \Delta V_1\rangle_{\text{tA}}/V$. Further, using $\langle \Delta V_1\rangle_{\text{tA}} = 0.5k\langle \Delta V_2\rangle_{\text{tA}}$ and $\langle v'_s(s_1)v'_s(s_2)\rangle_{\text{tA}} = 0$ ($\varepsilon_2 = 0$), we have

$$\eta = \frac{C_T}{C_P} = \frac{1}{1 + 0.5(1+\varepsilon_3)\langle \Delta V_2\rangle_{\text{tA}}/V} \tag{31}$$

where the relative velocity increment far downstream is

$$\langle \Delta V_2\rangle_{\text{tA}}/V = k^{-1}\left(\sqrt{1 + kC_T/e_{\text{flap}}} - 1\right) \tag{32}$$

In a special case where $k = 1$, $\varepsilon_3 = 0$ and $e_{\text{flap}} = 1$, Eq. (31) is reduced to the efficiency of an ideal propeller [3]. The parameter $k = 1 + 2r$ mainly describes the combined effect of the azimuthal velocity fluctuation and viscous shear stress. The parameter $\varepsilon_3 = \langle \Delta V_2\rangle_{\text{tA}}^{-2}\langle |v'|^2\rangle_{\text{tA}}(s_2)$ is the normalized total fluctuating kinetic energy far downstream.

Figure 3 shows the flapping propulsive efficiency as a function of the thrust coefficient C_T for different values of the flapping span efficiency in comparison with the ideal propeller efficiency when $k = 1$ and $\varepsilon_3 = 0.5$. The flapping span efficiency directly affects the flapping propulsive efficiency; a higher flapping span efficiency leads to a higher propulsive efficiency. For a bird whose flapping span efficiency is $e_{\text{flap}} = 0.463$, the propulsive efficiency ($\eta =$ 0.65–0.9) is less than that of an ideal propeller, but comparable to that of a practical propeller. Figures 4 and 5 show the effects of the parameters k and ε_3 on the flapping propulsive efficiency, respectively. Clearly, the propulsive efficiency is more sensitive to the normalized total fluctuating kinetic energy ε_3 than the parameter k representing the combined effect of the azimuthal velocity fluctuation, nonuniformity of velocity, and shear stress. The flapping

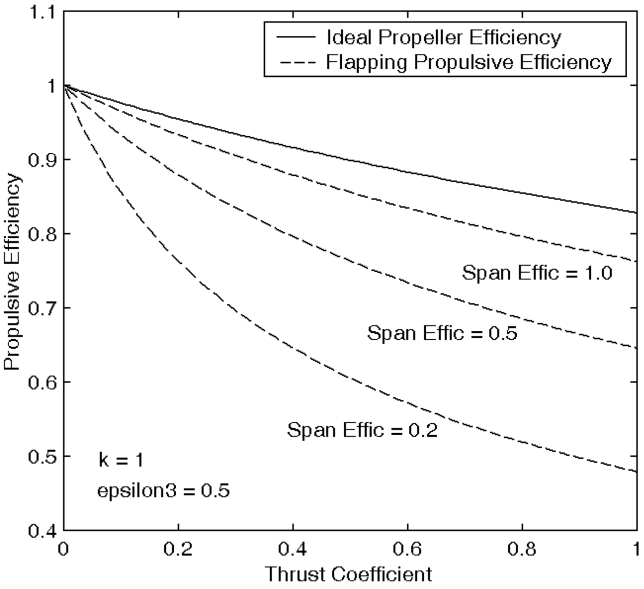

Fig. 3 The flapping propulsive efficiency as a function the thrust coefficient for different values of the flapping span efficiency.

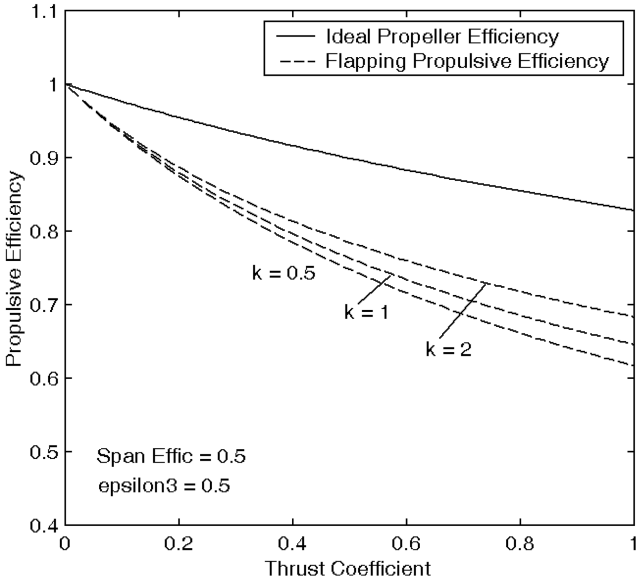

Fig. 4 The flapping propulsive efficiency as a function the thrust coefficient for different values of the parameter *k*.

propulsive efficiency decreases as the total fluctuating kinetic energy increases. Furthermore, the power coefficient in Eq. (32) can be rewritten as $C_T = 4C_{T(S_W)}/(\pi AR)$, where $C_{T(S_W)}$ is the power coefficient normalized based on the wing area S_W and AR is the wing aspect ratio. Hence, it can be seen that a larger wing aspect ratio improves the propulsive efficiency.

Using the scaling laws $V_{\text{mr}} = 8.98W^{1/6}$, $S_{\text{wing}} = 0.0327W^{2/3}$, and $P_{\text{mr,bird}} = 1.23W^{7/6}$ [26], we can estimate the propulsive efficiency for bird cruise flight, that is, $\eta_{\text{prop}} = V_{\text{mr}}D/P_{\text{mr}} = 9.62\rho C_{D,S_{\text{wing}}}$. For the air density $\rho = 1.21$ kg/m^3, we know $\eta_{\text{prop}} = 11.64C_{D,S_{\text{wing}}}$. As estimated before, the mean total drag coefficient of birds is $C_{D,S_{\text{wing}}} = C_{D_{\text{Para}},S_{\text{wing}}} + C_{D_{\text{In}},S_{\text{wing}}} = 0.076$ and therefore the propulsive efficiency of bird flight is $\eta_{\text{prop}} = 0.88$ that is in the range estimated by the MST model. An unsteady lifting-line theory gave the propulsive efficiency of 69–76% [17] and a theoretical model based on prescribed wake vortex structures constrained by minimum induced power requirements gave the efficiency as high as 86% [19,20].

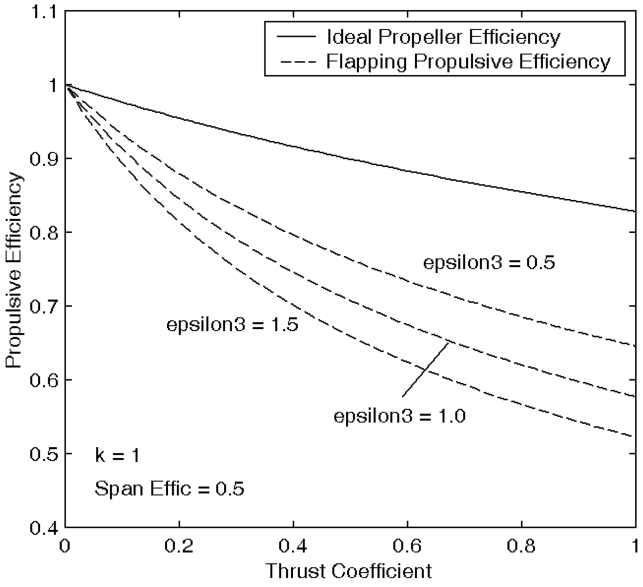

Fig. 5 The flapping propulsive efficiency as a function the thrust coefficient for different values of the parameter ε_3.

Conclusions

According to the time-area-averaged momentum stream tube model, the time-area-averaged power required for flapping flight is expressed as a superposition of the parasite (zero-lift) power and induced power similar to that given by the classical lifting-line theory for fixed-wing flight. For fast flapping flight, the temporal unsteadiness and spatial nonuniformity of velocity do not significantly affect the functional relation for the time-area-averaged power. A subtle but important difference in the power relation is that the flapping span efficiency has a different physical meaning from the Oswald efficiency for fixed-wing flight. The flapping span efficiency, nominally defined as a ratio between the effective actuator disk area and full circular area of a diameter of the wingspan, depends on the wing geometry (morphology) and flapping kinematics. The flapping propulsive efficiency is directly affected by the flapping span efficiency and normalized total fluctuating kinetic energy. A higher flapping span efficiency leads to a higher propulsive efficiency, whereas the flapping propulsive efficiency decreases as the normalized total fluctuating kinetic energy increases. When this model is used to fit the collected data for birds, the scaling relations for the cruise velocity and power of birds are obtained, and the flapping span efficiency, parasite, and induced drag coefficients and propulsive efficiency are estimated.

References

[1] Von Mises, R., *Theory of Flight*, Dover, New York, 1959, Chap. XII.
[2] Glauert, H., *The Elements of Aerofoil and Airscrew Theory*, 2nd ed., Cambridge University Press, Cambridge, 1993, Chap. XV.
[3] McCormick, B. W., *Aerodynamics of V/STOL Flight*, Dover, New York, 1999, Chap. 4.
[4] Leishman, J. G., *Principles of Helicopter Aerodynamics*, Cambridge University Press, Cambridge, U.K., 2000, Chap. 2.
[5] Horlock, J. H., *Actuator Disk Theory*, McGraw–Hill, New York, 1978, Chap. 3.
[6] Spalart, P. R., "On the Simple Actuator Disk," *Journal of Fluid Mechanics*, Vol. 494, Nov. 2003, pp. 399–405.
[7] Ellington, C. P., "The Aerodynamics of Hovering Insect Flight, Part V: A Vortex Theory," *Philosophical Transactions of the Royal Society of London, Series B: Biological Sciences*, Vol. 305, No. 1122, 1984, pp. 115–144.
[8] Templin, R. J., "The Spectrum of Animal Flight: Insects to Pterosaurs," *Progress in Aerospace Sciences*, Vol. 36, No. 5, 2000, pp. 393–436.
[9] Pennycuick, C. J., *Bird Flight Performance: A Practical Calculation Manual*, Oxford University Press, Oxford, 1989, Chap. 3.
[10] Sane, S. P., "Induced Airflow in Flying Insects," *Journal of Experimental Biology*, Vol. 209, Oct. 2006, pp. 32–42.
[11] Lighthill, J., "Introduction to the Scaling of Aerial Locomotion," *In Scale Effects in Animal Locomotion*, edited by T. J. Pedley, Academic Press, New York, 1977, pp. 365–404.
[12] Greenewalt, C. H., "The Flight of Birds," *Transactions of the American Philosophical Society*, Vol. 65, Pt. 4, 1975, pp. 1–67.
[13] von Holst, E., and Kuchemann, D., "Biological and Aerodynamical Problems of Animal Flight," *Journal of the Royal Aeronautical Society*, Vol. XLVI, No. 374, 1942, pp. 39–56.
[14] Jones, R. T., "Wing Flapping with Minimum Energy," *Aeronautical Journal*, Vol. 84, July 1980, pp. 214–217.
[15] Archer, R. D., Sapuppo, J., and Betteridge, D. S., "Propulsion Characteristics of Flapping Wings," *Aeronautical Journal*, Vol. 83, Sept. 1979, pp. 355–371.
[16] Betteridge, D. S., and Archer, R. D., "A Study of the Mechanics of Flapping Wings," *Aeronautical Quarterly*, Vol. 25, May 1974, pp. 129–142.
[17] Phlips, P. J., East, R. A., and Pratt, N. H., "An Unsteady Lifting Line Theory of Flapping Wings with Application to the Forward Flight of Birds," *Journal of Fluid Mechanics*, Vol. 112, Nov. 1981, pp. 97–126.
[18] Rayner, J. M. V., "A Vortex Theory of Animal Flight, Part 2. The Forward Flight of Birds," *Journal of Fluid Mechanics*, Vol. 91, Part 4, 1979, pp. 731–763.
[19] Hall, K. C., and Hall, S. R., "Minimum Induced Power Requirements for Flapping Flight," *Journal of Fluid Mechanics*, Vol. 323, Sept. 1996, pp. 285–315.
[20] Hall, K. C., and Hall, S. R., "A Rational Engineering Analysis of the Efficiency of Flapping Flight," in *Fixed and Flapping Wing Aerodynamics for Micro Air Vehicle Applications*, Vol. 195, edited by Thomas J. Mueller, Progress in Astronautics and Aeronautics, AIAA Press, Reston, VA, 2001, Chap. 13.
[21] Rayner, J. M. V., "Form and Function in Avian Flight," *Current Ornithology*, Vol. 5, Jan. 1988, pp. 1–77.
[22] Rayner, J. M. V., "On Aerodynamics and Energetics of Vertebrate Flapping Flight," in *Fluid Mechanics in Biology*, edited by A. Y. Cheer, and C. P. van Dam, Vol. 141, Contemporary Mathematics, American Mathematical Society, Providence, RI, 1992, pp. 351–400.
[23] Spedding, G. R., Rosen, M., and Hedenstrom, A., "A Family of Vortex Wakes Generated by a Thrush Nightingale in Free Flight in a Wind Tunnel over Its Entire Natural Range of Flight Speeds," *Journal of Experimental Biology*, Vol. 206, No. 14, 2003, pp. 2313–2344.
[24] Steiger, M. H., and Bloom, M. H., "Linearized Viscous Free Mixing with Streamwise Pressure Gradients," *AIAA Journal*, Vol. 2, No. 2, 1964, pp. 263–266.
[25] Anderson, J. D., *Fundamentals of Aerodynamics*, 2nd ed., McGraw–Hill, New York, 1991, Chap. 5.
[26] Liu, T., "Comparative Scaling of Flapping- and Fixed-Wing Flyers," *AIAA Journal*, Vol. 44, No. 1, 2006, pp. 24–33.
[27] Tennekes, H., *The Simple Science of Flight*, The MIT Press, Cambridge, MA, 1998, Appendix.
[28] Rayner, J. M. V., "Thrust and Drag in Flying Birds: Applications to Birdlike Micro Air Vehicles," in *Fixed and Flapping Wing Aerodynamics for Micro Air Vehicle Applications*, edited by T. J. Mueller, AIAA, Reston, VA, 2001, Chap. 11.